OH-Stretching Red Shifts in Bulky Hydrogen-Bonded Alcohols: Jet Spectroscopy and Modeling

Christine Cézard, Corey A. Rice, and Martin A. Suhm*

Institut für Physikalische Chemie, Universität Göttingen, Tammannstr. 6, 37077 Göttingen, Germany

Received: February 17, 2006; In Final Form: June 14, 2006

The available database for OH-stretching bands of jet-cooled aliphatic alcohol dimers is extended to systems including 1-adamantanol and 2-adamantanol, using a heated pulsed nozzle coupled to an FTIR spectrometer. This database is used to simplify and parametrize the standard Wang et al. AMBER/parm99.dat force field for the prediction of hydrogen-bond-induced red shifts, as it avoids complications due to mode coupling and cooperativity. Apart from subtle chiral recognition effects, the performance of the simple model in describing steric, electronic, and conformational influences on the red shifts is remarkable, as exemplified by predictions for mixed-alcohol dimers. The resulting semiempirical approach can complement quantum chemical calculations, in particular for larger systems, although the good performance is rather specific to red shift predictions.

1. Introduction

When two different alcohol molecules form a hydrogen-bonded dimer, there will be a preferential choice of the proton donor and acceptor positions. A probe for these O−H···O hydrogen bond interactions is the bathochromic shift (red shift) of the donor O−H stretching vibration.[1,2] In a simple picture, the "best" acceptor is presumably the one that induces the largest red shift, but the shift also depends in a nontrivial way on the donor molecule itself.[3] Infrared spectroscopy is the method of choice to study such red shifts,[4,5] but interpreting the resulting spectra is not always straightforward, as the chosen alcohol molecules often show conformational and configurational isomerism.[6−8] To calculate the vibrational spectrum of a cluster, a potential energy hypersurface is needed, which includes both intramolecular and intermolecular interactions. Accurate quantum mechanical methods to predict and interpret infrared spectra are computationally demanding, in particular, when they include anharmonicity. Molecular mechanics force fields are much less demanding and may provide a first hint for spectral assignments, if they are properly validated for this application. The Wang et al. AMBER/parm99.dat force field[9] and its successors[10] give reliable results concerning the structure, energetics, and intermolecular interactions of alcohols, but discrepancies are still found concerning intramolecular vibrational frequencies: this is not too surprising considering the simple way in which the intramolecular force field is parametrized. The prediction of wavenumber shifts in the intramolecular modes caused by intermolecular interactions is even more delicate. Therefore, one cannot expect a satisfactory performance of simple force fields in a strongly coupled situation involving intra- and intermolecular interactions.

Here, we want to investigate the power and limits of the Wang et al. AMBER force field[9] in a regime where it has the potential to perform satisfactorily. We choose aliphatic monofunctional alcohols. For their well-localized O−H stretching modes, it seems worthwhile to explore the potential of "reparametrized" force fields. We concentrate on hydrogen-bonded dimers, thus avoiding issues such as strong polarization and intermolecular mode coupling.

Several attempts to compute vibrational frequencies and/or red shifts in simple systems with force field methods have already been made. Derreumaux et al.[11−13] tested and enhanced several force fields in order to obtain the vibrational frequencies of a series of alkanes. Similar approaches have been applied to alcohols.[14] Buck et al.[15] used decoupled inter- and intramolecular model potentials for methanol clusters, based on OPLS[16] for the intermolecular part and on the anharmonic self-consistent field (SCF) force field of Schlegel et al.[17] for the intramolecular part. Parameters of the latter were fitted to experimental values to reproduce frequencies of the methanol monomer.

The main goal of this article is to test the reliability of the standard AMBER force field (i.e., the Wang et al. force field, using the parm99.dat[9] parameter set, without explicit polarization or explicit lone pairs on the oxygen atoms) to describe the O−H stretching vibrations in alcohol dimers. To this purpose, we will focus our attention on some simple aliphatic alcohols such as methanol (MeOH), ethanol (EtOH), 1-octanol (1-OctOH), propan-2-ol (2-PrOH), pentan-3-ol (3-PeOH), *tert*-butyl alcohol (*t*-BuOH), *tert*-butyldimethylcarbinol (tBdMOH), 1-adamantanol (1-AdaOH), and 2-adamantanol (2-AdaOH). All these alcohols have been investigated in our group by means of FTIR spectroscopy in the O−H stretching range and have been combined in different ways to test their donor/acceptor preferences. Experimental spectra of $(MeOH)_n$,[3,4,18] $(EtOH)_n$,[18,19] $(t\text{-}BuOH)_n$,[20] $(2\text{-}PrOH)_n$,[21] $(tBdMOH)_n$[22] with $n = 1$ or 2, and selected mixed dimers of these species have been presented in the past, whereas those of $(1\text{-}OctOH)_n$, $(3\text{-}PeOH)_n$, $(1\text{-}AdaOH)_n$, $(2\text{-}AdaOH)_n$, and mixed dimers MeOH-1-OctOH, MeOH-1-AdaOH, and 2-AdaOH-1-AdaOH are given here.

The present paper is organized as follows. Section 2 summarizes the experimental setups used to obtain the vibrational frequencies of hydrogen-bonded dimers as well as the theoretical methods used. Section 3 deals with the experimental results obtained on 1-OctOH, 3-PeOH, 1-AdaOH, 2-AdaOH, and the MeOH-1-OctOH, MeOH-1-AdaOH, and 2-AdaOH-1-AdaOH mixed dimers. In section 4, the Wang et al. AMBER force field[9]

* msuhm@gwdg.de.

10.1021/jp0610362 CCC: $33.50 © 2006 American Chemical Society
Published on Web 07/20/2006

with our minor reparametrization is tested for alcohol monomers and pure dimers. The available experimental values help in refining selected parameters of the force field. Section 5 focuses on mixed-alcohol dimers, thus showing the predicting power of the improved force field. Section 6 proposes a simplified protocol for the prediction of alcohol dimer OH red shifts, and section 7 summarizes our conclusions.

2. Methods

2.1. Experimental Apparatus. Mixed and pure hydrogen-bonded dimers of volatile alcohols up to 1-OctOH were generated in room-temperature pulsed supersonic slit jet expansions and probed via FTIR spectroscopy by synchronized interferometer scans. A large vacuum buffer (23 m^3) keeps the background pressure low during the gas pulse. Details of the jet FTIR spectrometers employing 120-mm- and 600-mm-long slit jet expansions used for this purpose are given elsewhere.[4,23]

Supersonic jet IR spectra of the O−H stretching vibrations of 1-adamantanol (99%, Sigma-Aldrich), 2-adamantanol (97%, Sigma-Aldrich), and their mixtures with MeOH seeded in He were recorded using a new heatable nozzle jet FTIR variant. In brief, a gas pulse is vertically expanded through a 5 mm × 1 mm slit nozzle into a 11 m^3 buffer chamber and probed perpendicularly by one to three 2 cm^{-1} scans of a Bruker IFS 66v/S FTIR spectrometer. It is equipped with a tungsten source, a CaF_2 beam splitter, and an optical filter (2.5−3.5 μm). The collimated IR beam is focused and recollimated with two CaF_2 lenses of 105 mm focal length inside the jet chamber. A parabolic mirror focuses the IR light onto a large area InSb detector, which is located in an external, evacuated detector chamber.

The gas expansion of 170−670 ms duration is controlled by a fast responding magnetic valve of 8 mm nominal width (Parker Lucifer) in combination with a pulse generator (Iota One, Parker). Between the magnetic valve and the slit nozzle, the gas flows through a resistively heated pick-up cell containing the 1-adamantanol and/or 2-adamantanol. The cell is enclosed by two check valves (Swagelok, SS-8CP2-1 and SS-8CP2-10) with differential opening pressures of 70 and 680 mbar. This ensures that molecules do not escape the cell between pulses. The evacuated buffer volume is pumped by a series of roots blowers at 2000 $m^3 \cdot h^{-1}$. After a recovery period of ca. 6−18 s per pulse, the process is repeated, and the resulting spectra are coadded. The stagnation pressure in the reservoir is 1.5 bar and consists of He (≥99.996%, Messer) or a mixture of He and MeOH (≥99.5%, Merck).

2.2. The AMBER Force Field. We used the Wang et al. parm99.dat[9]AMBER force field to perform normal-mode analysis on the different alcohol dimers. The force field is based on the following functional form:

$$E_{\text{total}} = \sum_{\text{bonds}} K_d(d - d_{eq})^2 + \sum_{\text{angles}} K_\theta(\theta - \theta_{eq})^2 + \sum_{\text{dihedrals}} \frac{V_n}{2}[1 + \cos(n\omega - \gamma)] + \sum_{\text{vdW}}^{i<j}\left[\frac{A_{ij}}{d_{ij}^{12}} - \frac{B_{ij}}{d_{ij}^{6}}\right] + \sum_{\text{elec}}^{i<j}\frac{q_i q_j}{\epsilon d_{ij}}$$

E_{total} represents the total potential energy for a given set of coordinates. The first two terms represent the energy associated with changes in bond lengths d and angles θ, respectively. The parameters d_{eq} and θ_{eq} are equilibrium bond lengths and bond angles, and K_d and K_θ are force constants (in fact, 0.5 times the standard force constants). The third term is the torsional term where V_n is the energy barrier of torsional motion, n is the periodicity, and γ is the phase. The last two terms represent the nonbonded interactions, the van der Waals and electrostatic components, respectively; A_{ij} and B_{ij} are the van der Waals parameters and q_i and q_j are the atomic charges.

Energy minimizations as well as vibrational analyses were carried out using the NMODE module of the *AMBER8* suite of programs.[24] Energy minimizations were done using a Newton−Raphson algorithm until the rms energy gradient was smaller than 10^{-5}. The vibrational normal modes were then calculated by diagonalizing the second derivative of the energy with respect to the mass-weighted Cartesian coordinate displacements relative to the minimum structure.

The General Amber Force Field (GAFF)[25] might have been an obvious choice for our study as it has been designed to model a large variety of organic molecules. But calculations performed on some alcohols (MeOH, *t*-BuOH) gave unsatisfactory results compared to our experimental ones and would have required major adjustment. These discrepancies may be related to an unusually low valence force constant for the O−H bond in the GAFF force field. The Wang et al.[9] force field provided us with a closer and more consistent first-order description according to our FTIR spectra.

As the main goal of this modeling is to predict the donor O−H stretching shifts, the only parameters of the force field we will reparametrize are the O−H bond force constants K_d and the charges (q_i, q_j) on the bonding atoms. The original Wang et al. AMBER parameters in parm99.dat[9] for equilibrium bond lengths are taken from experimental results on appropriate compounds, whereas the bond force constants often derive from ab initio calculations. Approximations inherent to the representation of the force field and a desire to maintain as much transferability as possible among compounds of the same kind preclude a precise fitting for small organic molecules. Hence, only the general features of the vibrational spectra are reproduced, such as an O−H stretching vibration of ca. 3709 cm^{-1}, independent of the alcohol monomer studied. However, the implementation of the force field into the AMBER program makes it possible to "tune" the bond stretching force constants for small molecules.

Ab initio calculations other than charge derivation (i.e., geometry optimizations and frequency calculations) were done using the *GAUSSIAN03*[26] program.

3. Experimental Results

3.1. 1-Adamantanol and 1-Adamantanol−Methanol. Figure 1 shows the spectra of pure 1-adamantanol and pure methanol as well as a mixture of methanol with 1-adamantanol. The spectrum of pure 1-adamantanol (Figure 1a) shows the dimer peak further red-shifted than the methanol dimer band (Figure 1b). This is a consequence of the electron-donating effects of the alkyl group, which soften the OH bond in the monomer and make it a better hydrogen bond acceptor in the dimer. Both effects have similar magnitude. In the mixed MeOH−1-AdaOH dimer with MeOH as the donor, only the latter effect is active. Therefore, one expects the donor stretching band to fall between the $(MeOH)_2$ and the $(1\text{-AdaOH})_2$ bands. We can observe this in the jet spectrum of the mixed complex (Figure 1c). A more quantitative analysis of red shifts in mixed-alcohol dimers can be found in ref 3.

3.2. 2-Adamantanol and 2-Adamantanol−1-Adamantanol. Figure 2 shows the spectrum of an expansion of 2-AdaOH (trace a) as well as a mixture of 2-AdaOH with 1-AdaOH (trace b). The monomer of 2-AdaOH (M_2) absorbs at a somewhat higher wavenumber than 1-AdaOH (M_1), as expected for a secondary

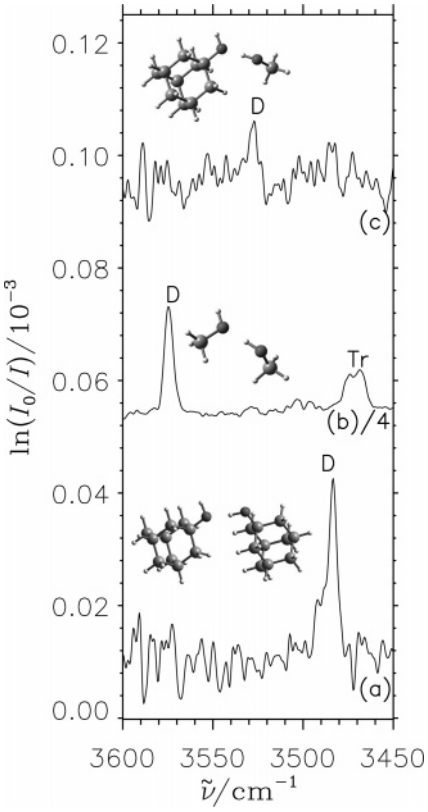

Figure 1. Donor OH-stretching spectra of jet expansions of pure 1-adamantanol (a), pure methanol (b) (ref 3, scaled by $^1/_4$), and a mixture of 1-adamantanol with methanol (c). Dimer peaks are marked D along with AMBER minimum structures. In the case of methanol, a trimer transition (Tr) is also seen.

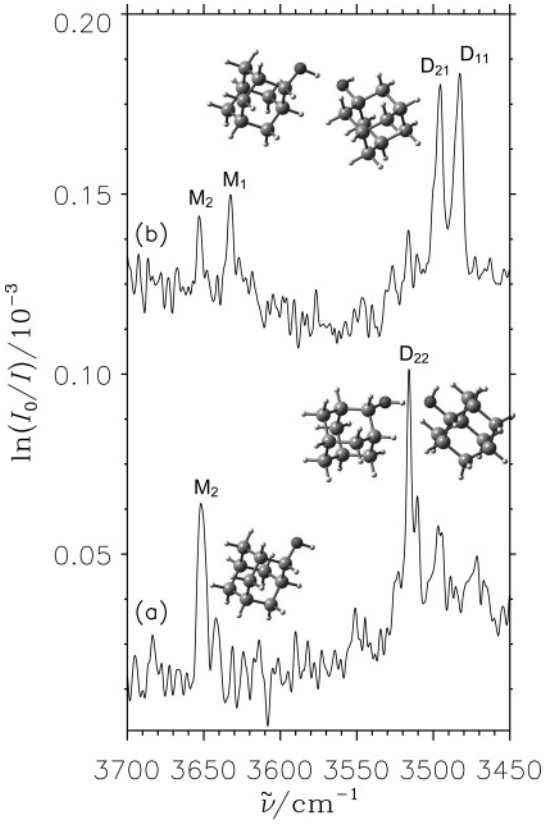

Figure 2. OH-stretching spectra of jet expansions of pure 2-adamantanol (a) and a mixture of 2-adamantanol with 1-adamantanol (b). Monomer and dimer donor peaks are marked M_i and D_{ij}, respectively, along with AMBER minimum structures for D_{22} and D_{21} (index 1 for 1-adamantanol and index 2 for 2-adamantanol). The nozzle temperature at which the substances were expanded was 423 K.

alcohol with reduced inductive effect. A single absorption peak is consistent with the prediction that the OH group is located gauche relative to the adjacent C−H group. Ab initio RHF/6-31G* and RHF/6-21G, as well as AMBER calculations, confirm the gauche conformer to be the most stable. The dimer OH stretch of 2-AdaOH (D_{22}) is also less red-shifted than that of 1-AdaOH (D_{11}) as a consequence of the reduced inductive effect. Only one prominent band is observed and may be tentatively attributed to one or more of the four possible gauche−gauche forms with identical or opposite chirality.[18] When 1-AdaOH is added to the heated compartment (trace b), both monomers are observed, and D_{22} is depleted in favor of a mixed-dimer peak D_{21} intermediate in frequency between D_{22} and D_{11}.

3.3. Pentan-3-ol. The monomer and dimer of pentan-3-ol were detected more conventionally using the 600 mm jet FTIR spectrometer.[23] 0.05% of pentan-3-ol (98%, Aldrich) was expanded in He at 0.6 bar. Figure 3 shows the resulting spectrum. The lower trace results from a gas-phase measurement at 298 K and exhibits a broad monomer OH-stretching peak. Its fine structure is indicative of conformational isomerism. The upper trace shows the jet spectrum, in which the monomer peak is more narrow but may still contain contributions from more than one conformation. In the absence of a rotationally resolved spectrum and conformational analysis, we locate the band center close to the dip between the two peaks. Shifted by $-\Delta\tilde{\nu}_{OH}$ to lower wavenumber, a sharp dimer OH donor peak emerges. Here, conformational isomers seem to play only a minor role. The peak position compares well with our earlier 120 mm jet FTIR measurement[4] at a much higher concentration. Therefore, other dimer band positions were taken from that work[4] and subsequent studies.[18,20−22]

3.4. 1-Octanol and Methanol−1-Octanol. Although long-chain alcohols potentially show rich conformational isomerism, we have also recorded spectra of 1-OctOH expansions and 1-OctOH-MeOH coexpansions, displayed in Figure 4. Quite surprisingly, the 600 mm jet spectrum of 1-OctOH shows a single sharp monomer peak (M_O in trace a), which is located at the high-frequency end of a number of gas-phase absorptions due to different thermally populated conformers. Exploratory calculations up to MP2/6-311+G* level indicate that it corresponds to a trans −OH conformation relative to the backbone C−C bond. While the energy difference to the gauche conformation is small and not uniform in sign, the trans conformation is consistently predicted to be more blue-shifted. The dimer region is indicative of substantial isomerism, but again, the most blue-shifted transition is expected to involve trans octanol monomers. When MeOH is added to the expansion (trace b), both monomers are observed, and a prominent peak between MeOH dimer (D_M) and 1-OctOH dimer (D_O) is likely to have a MeOH−1-OctOH origin (D_{MO}). A detailed assignment will require more systematic investigations, but the case of 1-OctOH can serve as a further primary alcohol test case for the AMBER model already at this stage.

4. Spectroscopic Testing of the AMBER Force Field

To test the ability of the Wang et al. AMBER force field[9] to reproduce and predict IR spectra, calculations are performed on a set of alcohol systems for which experimental monomer and dimer spectra have been recorded using jet FTIR spectroscopy. They will also be compared to low-level ab initio calculations (RHF/6-21G) which employ an approach that has

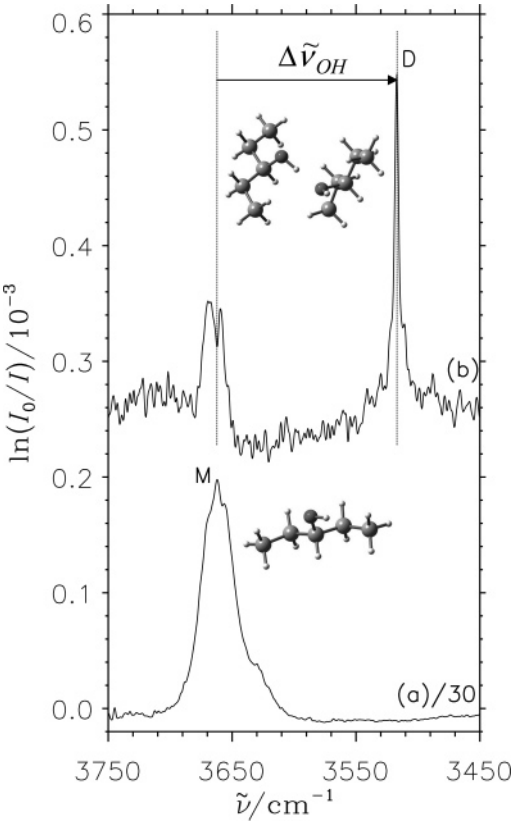

Figure 3. OH-stretching spectra of pentan-3-ol in He in the 298 K gas phase (a) and in a supersonic jet expansion (b), showing monomer (M) and dimer donor (D) bands.

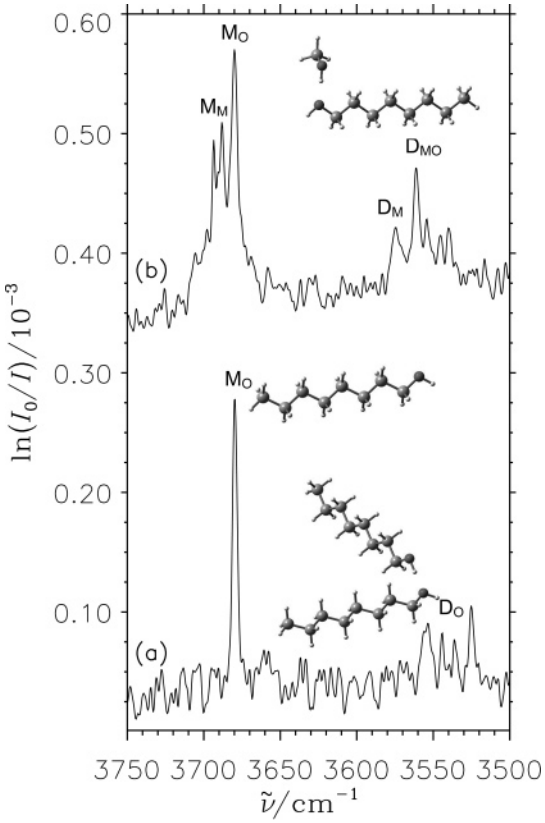

Figure 4. Donor OH-stretching spectra of jet expansions of pure 1-octanol (a) and of a mixture of 1-octanol with methanol (b). Monomer and dimer peaks are marked M and D, respectively, along with AMBER minimum structures (index O for 1-octanol and index M for methanol).

been empirically found by us to give a satisfactory performance for alcohol dimer red shifts. In this context, it should be noted that only high-level ab initio calculations are expected to provide reasonably accurate vibrational red shifts.[18] MP2 calculations are not yet feasible for large systems. B3LYP calculations predict the correct order of magnitude but fail qualitatively for the most elementary alkyl substitution test.[20] HF calculations predict red shifts of insufficient magnitude. To obtain the right order of magnitude at HF level (at the price of overestimated binding energies), one has to introduce basis set superposition errors by the choice of a small basis set. In exploratory calculations, we found the almost minimal HF/3-21G basis set to provide reasonable relative trends,[20] whereas the somewhat larger HF/6-21G basis set even predicts red shifts which come close to the experimental values in absolute terms, obviously due to substantial error compensation.

Vibrational frequencies were computed for all the alcohol monomers using the Wang et al./parm99.dat[9] force field parameters. This study used the RESP method[27−29] (Restrained ElectroStatic Potential fit) to calculate initial atomic charges. The basic idea with electrostatic potential fit charges is that a least-squares fitting algorithm is used to derive a set of atom-centered point charges which best reproduce the electrostatic potential of the molecule. The charge-derivation process was started by calculating the electrostatic potential for the optimized alcohol monomer using the *GAMESS* program[30] at the RHF/6-31G* level of theory. A RESP fit was then carried out on one or more conformations, depending on the complexity of the alcohol studied, in two stages using the RESP tool of the *AMBER8* program suite.[24] The fit was performed according to the standard procedure described in refs 27−29 using the Connolly algorithm and without introducing any intramolecular constraints other than that the structurally equivalent atoms within a monomer were forced to have identical charges in the second RESP stage. We followed this procedure for all the alcohols except for the monomer of methanol, where the charges have been taken from the article of Cieplak et al.[31] The initial and complete sets of charges for all the alcohols are summarized in Figure 5 and in Table 1 for the charges on the hydroxyl group. One can observe that the charges on the hydroxyl hydrogen are nearly the same for all the alcohols, i.e., around +0.42 e. As the default force constants are used for all these primary calculations, the same O−H-stretching wavenumber (3709 cm^{-1}) is obtained for all alcohol monomers. The default K_{OH} value[32] is 553.0 kcal·mol^{-1}·Å^{-2}, and it has been calibrated to sugars, tyrosine, and serine. Using experimental monomer O−H stretching-wavenumbers, an individual K_{OH} force constant was then adjusted for each monomer conformation. We should note that this adjustment has essentially no consequences for the hydrogen-bond-induced shifts and is only carried out for reasons of consistency. Obviously, it mimics anharmonic oscillators with an effective harmonic potential. This is based on the observation that anharmonicities are not severely affected by moderate OH···O hydrogen bonds, but it has consequences for the coupling which will be discussed below. Table 1 summarizes the results thus obtained and compares them to the FTIR measurements on the monomers. The gauche/trans nomenclature refers to the unique substituent where all three substituents are not the same. In some cases, the different alcohol conformations give rise to distinct IR absorptions,[18] but more typically, the bands overlap, and the exact conformational assignment remains open. Test calculations and experimental data[18,33] indicate that in most cases discussed in the present work, except for the case of primary alcohols, the gauche OH conformation is preferred over the trans conformation. However, our approach is quite

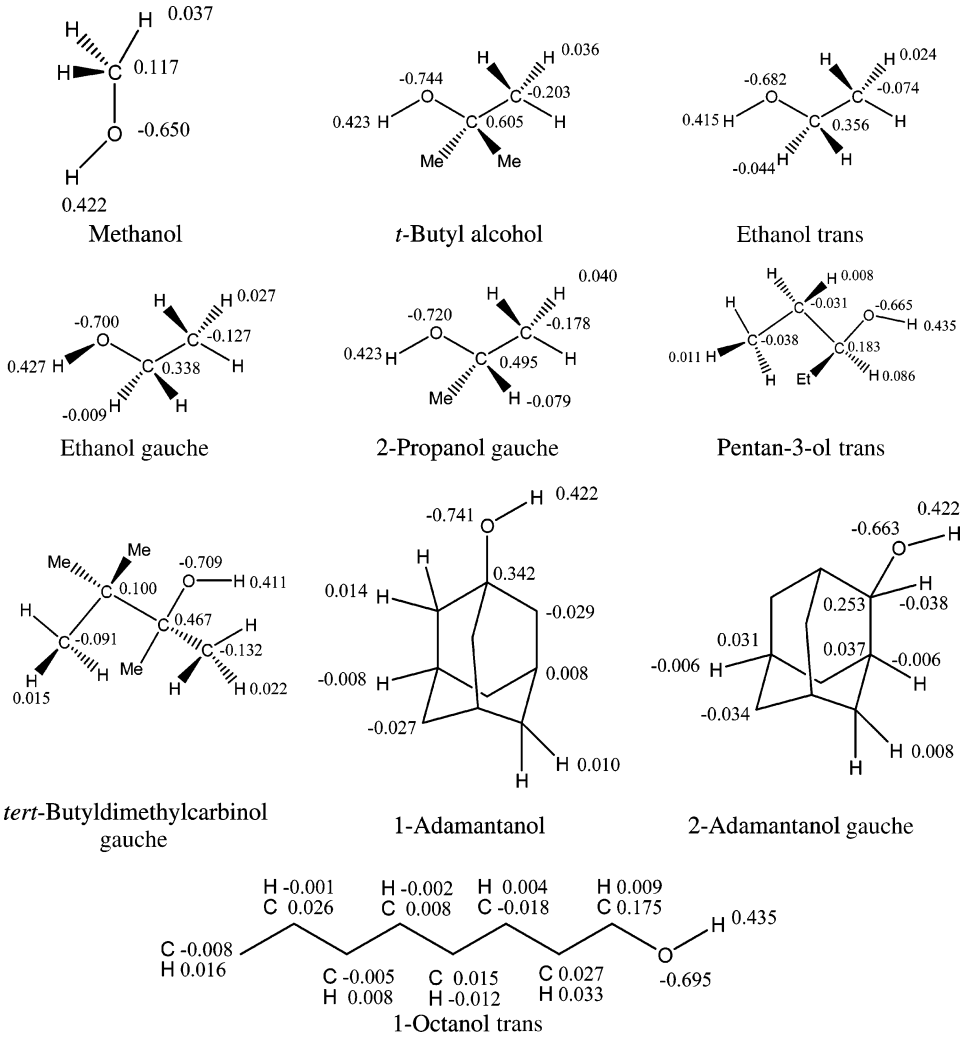

Figure 5. Initial charge models for the alcohols.

TABLE 1: Alcohol Monomers: Experimental O−H Stretching Wavenumbers (in cm^{-1}); Original Atom Charges δO, δH (in e); Adjusted Force Constants K_{OH} (in kcal·mol^{-1}·Å^{-2}); and Resulting AMBER Harmonic O−H Wavenumbers (in cm^{-1})

	exp	δO	δH	K_{OH}	AMBER
MeOH	3686[a,b,c]	−0.650	0.422	545	3683
EtOH gauche	3661[d]	−0.700	0.423	539	3662
EtOH trans	3678[d]	−0.682	0.415	543	3676
1-OctOH trans	3680	−0.695	0.435	544	3679
2-PrOH gauche	3658[e]	−0.720	0.423	538	3659
3-PeOH gauche	3661	−0.635	0.409	539	3663
3-PeOH trans	3661	−0.665	0.435	539	3663
3-PeOH multiconf		−0.548	0.360	539	3663
2-AdaOH	3653	−0.663	0.423	536	3652
t-BuOH	3643[b]	−0.744	0.423	534	3645
tBdMOH gauche	3650[a,f]	−0.709	0.411	535	3649
1-AdaOH	3634	−0.741	0.422	531	3635

[a] ref 4. [b] ref 3. [c] ref 43. [d] ref 18. [e] ref 21. [f] ref 22.

independent of the conformational monomer assignment, as long as the conformation is preserved in the dimer (vide infra).

All the pure alcohol dimers were then built and minimized using a Newton−Raphson method, and a normal-mode analysis was performed. The optimized dimer structures are shown in Figure 6, whereas the (harmonic) $\tilde{\nu}_{OH}$ wavenumbers are reported in Table 2 and compared to experimental (anharmonic) ones. Surprisingly, one can observe that, for the smaller alcohols, the donor O−H-stretching wavenumbers are in rather good agreement with those obtained experimentally. Dimer wavenumbers for larger alcohols are systematically overestimated.

The relatively satisfactory performance of the original Wang et al. AMBER force field[9] deserves a brief discussion. It is known that ab initio harmonic hydrogen-bond-induced red shift predictions generally profit from substantial error compensation. This is because there are (mostly diagonal) anharmonic contributions which increase the red shift as well as (mostly librational zero-point motion induced) anharmonic contributions which reduce the red shift.[5] However, the AMBER model suffers from an additional approximation which may be more critical. By modeling the monomer OH as a harmonic oscillator, it misses out all red shift contributions which originate from a linear perturbation of the oscillator. Such red shift contributions have been argued[34] to account for a major fraction of the total frequency shift. The fact the original AMBER prediction for the methanol dimer shift is nevertheless nearly perfect (112 cm^{-1} vs 111 cm^{-1}) can only be explained by an overestimation of the hydrogen bond perturbation. Indeed, the OH bond length is extended by about 0.03 Å in methanol, which is approximately three times the extension predicted by ab initio calculations.[35] In line with this threefold overestimate of the bond length extension, the electronic binding energy of methanol dimer in the AMBER model is about three times larger than the experimental zero-point energy corrected value of 13 kJ·mol^{-1} [36] or about two times larger than the true electronic binding energy. This overpolarization effect is actually exploited in the modeling

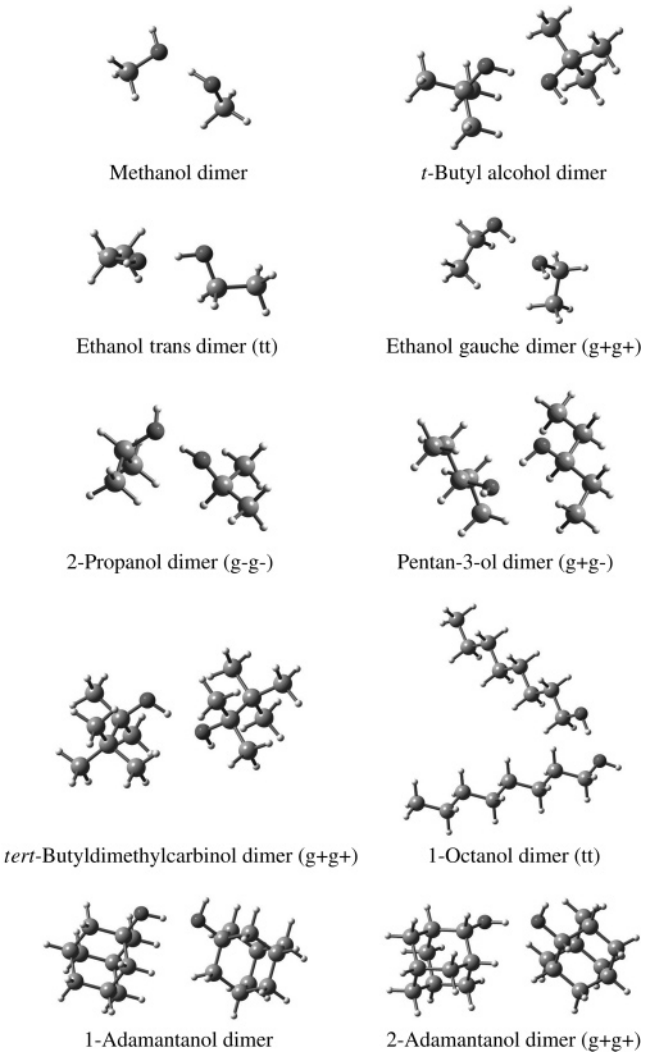

Figure 6. Most stable pure alcohol dimers. The OH g/t nomenclature is relative to the unique substituent at C_α.

of condensed phases with pairwise additive potentials, which lack the hydrogen bond strengthening mechanism beyond the dimer. It also helps in bringing the dimer red shifts into the experimental range, despite the neglect of anharmonic contributions to the OH-stretching potential. One should thus be aware of the massive error compensation underlying the AMBER performance for vibrational red shifts, which we exploit in the following semiempirical approach.

In this spirit, the initial prediction of hydrogen-bond-induced red shifts (set 1), based solely on a RHF/6-31G* RESP charges, forms the starting point for a sequence of simplifications and refinements. In a first step, the charges on O and H are kept, but all charges on nonfunctional atoms are collected in the carbon atom adjacent to the OH group. Setting all charges except for the C−O−H unit to zero a posteriori is not expected to affect the spectral prediction significantly, as the dominant interactions between alkyl groups are not electrostatic in nature. This expectation is confirmed in Table 2 (set 2). Indeed, the agreement with experiment fortuitously improves somewhat, with the bulky alcohols still showing the largest deviations. We have also verified that this simplification does not affect the structure and energetics of the hydrogen-bonded dimers. The second simplification is inspired by the observation that the charges on the hydroxyl hydrogen (*H*O) are very similar for all the alcohols. In set 3, we have therefore fixed them at +0.42 e for all the alcohols. The oxygen charge was kept at its original value, and the charge on the adjacent carbon was fixed in the same way as in set 2 to ensure electroneutrality. This leads to slightly larger deviations from the experimental values with the benefit of leaving only one charge parameter for each alcohol molecule. In a single refinement step following these simplifications, the oxygen charge was now adjusted to reproduce the experimental wavenumber shift for the alcohol dimer. The resulting optimum charges are reported in Table 3, along with set 1, set 2, and set 3. The O−H-stretching frequencies of the alcohol monomers were recomputed with these new sets of charges. As expected, the $\tilde{\nu}_{OH}$ wavenumbers are not affected by the charge adjustments by more than 0.1 cm^{-1}.

To check whether the frequency deviation observed for the most bulky alcohols could be due to a conformational effect, we did some more calculations on the pentan-3-ol monomer and dimer. As can be seen on the recorded spectrum in Figure 2, the monomer absorption shows a structured band, which means that more than one conformation of the pentan-3-ol monomer may be present in the jet. The dimer peak is sharp, indicating that only one dimer is formed. Ab initio calculations at the RHF/6-31+G* level predict that the trans and gauche forms are only separated by 1 kJ·mol^{-1}, in favor of the gauche one, but at the RHF/6-31G* level, actually used to compute the RESP charges, the trans monomer is slightly more stable. Such conformational energy differences are quite difficult to predict, even at considerably higher levels of electronic structure treatment.[6,18] As can be seen in Table 1, the charges on the hydroxyl group of the trans and gauche conformers of pentan-3-ol are different, leading to different red shifts upon dimerization as reported in Table 2. Although the results obtained with the charges computed on the trans conformer are closer to experiment, the optimized set of charges is independent of the starting conformation of the alcohol. Moreover, starting from our previous most stable dimer structure, we rotated the ethyl groups of each monomer (rotation around the $-(H_2)C-C(CH_2-CH_3)$ axis in steps of 10°), first individually and then together, minimized the thus obtained dimer and then performed a normal-mode analysis, both with the set 1 and set 3 charges. These structures all converged toward a few minima only. For every minimum, the frequency deviations observed are independent of the set of charges used, and moreover, these deviations are very small among the minima. When only one ethyl group is rotated, the induced shift is less than 1 cm^{-1}; when all four ethyls are rotated, the shift is less than 3 cm^{-1}.

Whenever the prevalent monomer conformations in the jet expansion remain unknown, the simple RESP procedure using a single conformation may be considered inadequate, and a procedure including more than one conformation may appear desirable. Table 1 shows the charges obtained on 3-PeOH after a RESP[28,29] multiconformational fit (trans and gauche 3-PeOH with an equal weight). The resulting charges differ significantly from the ones obtained after a monoconformational fit, and in this case, a poor O−H-stretching wavenumber upon dimerization is obtained (Table 2). Upon application of the charge simplification and optimization steps, the dependence on the employed RESP procedure is naturally removed, as long as conformations are not obvious from the spectra.

Upon dimerization, many of the alcohols show a gauche−gauche conformation. As the gauche monomer exists in two enantiomeric g+ and g− conformations, this leads to the formation of four spectroscopically distinguishable dimer conformations (vide infra). Independent of the charge set used, our AMBER calculations predict a unique red shift for these four kinds of dimers.

TABLE 2: Pure Alcohol Dimers: Donor O−H Stretching Wavenumbers $\tilde{\nu}_{OH}$ and Differences $\Delta\tilde{\nu}^{e}_{OH}$ to Experiment (in cm^{-1}) with Three Sets of Charges[a]

		set 1		set 2		set 3		opt. set	
	exp	$\tilde{\nu}_{OH}$	$\Delta\tilde{\nu}^{e}_{OH}$	$\tilde{\nu}_{OH}$	$\Delta\tilde{\nu}^{e}_{OH}$	$\tilde{\nu}_{OH}$	$\Delta\tilde{\nu}^{e}_{OH}$	$\tilde{\nu}_{OH}$	$\Delta\tilde{\nu}^{e}_{OH}$
$(MeOH)_2$	3575[b,c]	3571	−4	3574	−1	3575	0	3575	0
$(EtOH_{g+g+})_2$ gg[g]	3532[b,d,e]	3534	+2	3532	0	3538	+6	3530	−2
$(1\text{-OctOH})_2$	3554	3543	−11	3548	−6	3559	+5	3553	−1
$(2\text{-PrOH})_2$	3520 [f]	3530	+10	3526	+6	3527	+7	3520	0
$(3\text{-PeOH})_2$ gg[g]	3517	3569	+52	3566	+49	3561	+44	3516	−1
$(3\text{-PeOH})_2$ tt[g]	3517	3557	+40	3548	+31	3551	+34	3516	−1
$(3\text{-PeOH})_2$ m	3517	3602	+85	3602	+85	3582	+65	3516	−1
$(2\text{-AdaOH})_2$	3516	3541	+25	3539	+23	3542	+26	3515	−1
$(tBdMOH)_2$	3500	3537	+37	3532	+32	3525	+25	3503	+3
$(t\text{-BuOH})_2$	3497[b]	3511	+14	3503	+6	3507	+10	3499	+2
$(1\text{-AdaOH})_2$	3483	3509	+26	3509	+26	3495	+14	3483	0

[a] Set 1: Initial complete set of charges obtained via the RESP methodology at the RHF/6-31G* level of theory (except for methanol, see text). Set 2: Charges of all nonfunctional atoms are collected in the adjacent C−OH carbon atom. Charges on *O*H and *H*O have the same value as in set 1. Set 3: Same as in set 2, but now for all the alcohols, the *H*O charge is set to +0.42 e. The charge on the *O*H is still on its initial value. Opt. set: The charge on the *H*O is kept at +0.42 e; the charge on the *O*H is adjusted to closely reproduce the experimental value for the OH-stretching fundamental. [b] ref 4. [c] ref 3. [d] ref 18. [e] ref 19. [f] ref 21. [g] only refers to the monomer "geometry" charges, not to the actual structures. The actual structures may be found in Figure 6.

TABLE 3: Charges on the O and H Atoms

		set 1/set 2		set 3		opt. set	
subst		δO	δH	δO	δH	δO	δH
0	MeOH	−0.650	0.422	−0.65	0.42	−0.65	0.42
1	EtOH gauche	−0.700	0.427	−0.70	0.42	−0.72	0.42
1	1-OctOH	−0.695	0.435	−0.70	0.42	−0.71	0.42
2	2-PrOH	−0.720	0.423	−0.72	0.42	−0.74	0.42
2	3-PeOH	−0.665	0.435	−0.67	0.42	−0.76	0.42
2	2-AdaOH	−0.663	0.423	−0.66	0.42	−0.74	0.42
3	*t*-BuOH	−0.744	0.423	−0.74	0.42	−0.76	0.42
3	tBdMOH	−0.709	0.411	−0.71	0.42	−0.77	0.42
3	1-AdaOH	−0.741	0.422	−0.74	0.42	−0.77	0.42

All this indicates a certain robustness of our simple approach which concentrates on charges in the vicinity of the oxygen atom. This is useful, considering the remaining experimental uncertainties in the conformational assignment.

Figure 7 plots the correlation between experimental red shifts of the donor OH-stretching mode and the AMBER red shifts obtained upon dimerization for all the alcohols with set 1 and the optimized set of charges, as well as the correlation between experimental red shifts and ab initio harmonic RHF/6-21G ones. The predictions given by the RHF calculations fit quite well the experimental shifts (rms deviation of 16 cm^{-1}), although they tend to overestimate them a bit, whereas the AMBER predictions with the original charges (set 1) underestimate them (rms deviation of 22 cm^{-1}). Neither the RHF method nor the original AMBER force field (set 1) are able to predict the correct red shift sequence according to the experiment (MeOH < 1-OctOH < $EtOH_{g+g+}$ < 2-AdaOH < 2-PrOH < 3-PeOH < *t*-BuOH < tBdMOH < 1-AdaOH). In the simplified force field with adjusted oxygen charge, both oxygen charge and red shift show the qualitative increase from primary over secondary to tertiary alcohols and by construction reproduce the experimental data (rms of 3 cm^{-1}).

4.1. Dimers of Ethanol. Among the selected alcohols, ethanol represents a simple example of conformational isomerism. It exists in a trans (t) and two enantiomeric gauche (g+, g−) conformations, with the energetical balance between trans and gauche conformations being subtle.[37,38] From these three monomers, nine enantiomeric pairs of dimer conformations can be formed, in a simple picture.[18,21] These isomers can be easily enumerated when looking along the CCO backbone such that the O atom is pointing upward. Both the hydrogen donor and acceptor can adopt t, g+, and g− states, depending on whether the OH group points in the direction of the backbone, to its right, or to its left, respectively. The hydrogen-bonding H atom can attach to one of the two lone pairs of the acceptor oxygen. These are located on the right and on the left side of the directed OH bond. This leads to enantiomeric pairs which are spectroscopically indistinguishable. Therefore, we restrict the discussion to dimers engaging the right lone pair only. The nine resulting dimer conformations are tt, tg+, tg−, g+t, g−t, g+g+, g−g−, g−g+ and g+g−; tg+, for example, is a dimer with a trans donor ethanol hydrogen-bonded to the right-handed lone pair of a gauche+ ethanol acceptor.

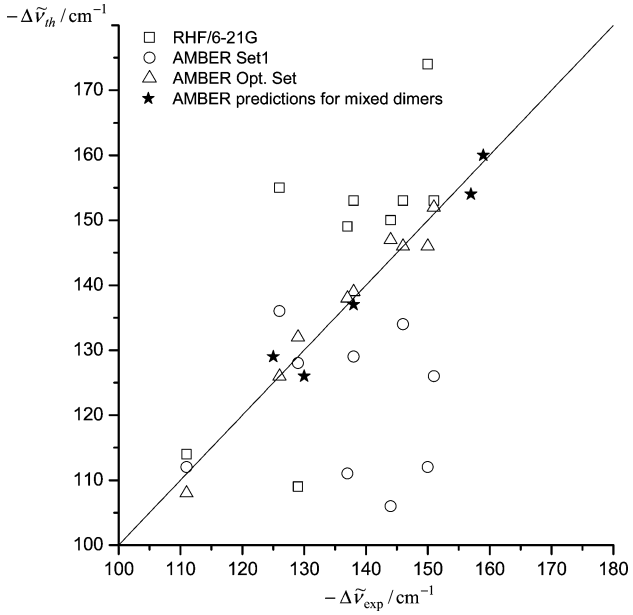

Figure 7. Correlation between experimental dimerization red shifts $-\Delta\tilde{\nu}_{exp}$ of the donor OH-stretching mode and simple ab initio predictions (□, RHF/6-21G, 16 cm^{-1} root-mean-square deviation (rms)), the original AMBER prediction (○, AMBER/set 1, refer to Table 2, rms deviation of 22 cm^{-1}), and the optimum AMBER parametrization (Δ, AMBER/opt. set, refer to Table 2, rms of 3 cm^{-1} by construction), $-\Delta\tilde{\nu}_{th}$. For the mixed-alcohol dimers (★), the correlation between the experimental red shifts of the donor stretching mode and the AMBER predictions (rms of 3 cm^{-1}) is also shown.

Experimentally, the jet FTIR OH-stretching spectrum shows the two monomers, a dimer and a trimer region, and it has been pointed out that the most red-shifted OH-stretching band belongs

TABLE 4: Charges on the O and H Atoms for the Ethanol Molecules

	set 1/set 2		set 3		opt. set	
	δO	δH	δO	δH	δO	δH
EtOH trans	−0.682	0.415	−0.68	0.42	−0.70	0.42
EtOH gauche	−0.700	0.427	−0.70	0.42	−0.72	0.42

TABLE 5: Ethanol Dimer $\tilde{\nu}_{OH}$ Wavenumbers (cm^{-1}) Depending on the Set of Charges[a]

	exp[b]	set 1	set 2	set 3	opt. set
g+g+	3532	3534.4	3532.4	3537.5	3530.2
g−g−	3539 ± 8	3534.3	3532.3	3537.3	3529.9
g−g+	3539 ± 8	3534.1	3532.2	3538.0	3529.8
g+g−	3539 ± 8	3535.0	3532.9	3537.9	3530.6
tt	3539 ± 8	3564.2	3562.4	3559.9	3552.8
tg+	3539 ± 8	3555.4	3553.3	3563.2	3541.9
tg−	3539 ± 8	3555.7	3553.5	3563.5	3542.1
g−t	3539 ± 8	3544.0	3542.3	3560.2	3541.1
g+t	3539 ± 8	3545.6	3543.9	3561.3	3542.5
spread	≥16	30	30	26	23

[a] Also shown is the spread of ethanol dimer transitions in cm^{-1}. Unlike individual non g+g+ transitions, it is already known experimentally. [b] ref 18.

to the g+g+ dimer.[18] Unlike pentan-3-ol, the peaks corresponding to the gauche and trans conformers have been clearly identified and assigned, and we can go beyond the simplifying approach suggested before in this special case. Hence, to distinguish the gauche conformation from the trans one in the AMBER force field, different charges and force constants can be used, as stated in Table 4. For charge and force constant optimizations, the same procedures as shown previously are used. There is no way to optimize the oxygen charge of the trans ethanol molecule, as no exact vibrational assignment is available for an ethanol dimer involving a trans donor and/or acceptor. We should note, however, that EtOH gauche − EtOH trans dimer structures have been identified by Hearn et al.[39] by means of FTMW spectroscopy. In analogy to gauche EtOH, we add −0.02 e on the original oxygen charge for trans EtOH for the "optimized" set. All ethanol dimer calculations, except for the g+g+ one, are thus predictions. Results are gathered in Table 5. A first remark is that AMBER predicts about the same position for the four gg conformations, which is not consistent with ab initio calculations of Emmeluth et al.[18] Subtle chiral recognition effects seem to be beyond the capabilities of the force field. This is confirmed by the fact that there is not much of a difference between a tg+ and a tg− conformation. The force field gives nearly the same wavenumbers for both of the conformations, which is also not consistent with the ab initio calculations of Emmeluth et al.[18] All other dimers are blue-shifted with respect to the g+g+ dimer, which is consistent with both experiment and theory. The frequency spread of the transitions is of the correct order of magnitude and improves with refinement. Although one should not overestimate the robustness of the AMBER approach for such subtle issues, we remark that the experimental bunching of the OH-stretching transitions into three more or less equidistant peaks is predicted quite well.

5. Mixed-Alcohol Dimers

In a second step, we built mixed-alcohol dimers, optimized their structure, and performed normal-mode analyses using the sets of charges defined before in a purely predictive approach. The first mixed dimer we will focus on is methanol−*tert*-butyl alcohol.

TABLE 6: OH-Stretching Wavenumber Predictions (in cm^{-1}) for Mixed Dimers Based on Original Charges (set 1), on C−O−H Collapsed Charges (set 2), and on Charges Calibrated on Pure Dimers (opt. set) Compared to Experiment (exp)

	exp.	set 1	set 2	opt. set
MeOH-*t*-BuOH	3529[a]	3545	3534	3529
t-BuOH-MeOH	*b*	3536	3541	3548
MeOH-1-AdaOH	3527	3536	3537	3523
1-AdaOH-MeOH	*b*	3527	3532	3533
MeOH-1-OctOH	3561	3554	3559	3554
1-OctOH-MeOH	*b*	3561	3564	3574
2-AdaOH-1-AdaOH	3496	3507	3506	3498
1-AdaOH-2-AdaOH	*b*	3537	3537	3509

[a] ref 3. [b] Not yet detected, as it converts to the more stable mixed dimer in the supersonic jet expansion.

5.1. MeOH/*t*-BuOH. This is one of the simplest cases of mixed-alcohol dimers. Indeed, these two alcohols do not show any torsional isomerism, which allows for a straightforward spectral interpretation.[18] Two dimers can be formed, i.e., MeOH as the donor and MeOH as the acceptor. The dimer with methanol as the donor is more stable[3] by about 2−4 kJ·mol^{-1}. The AMBER calculations predict a consistent energy difference of 3.4 kJ·mol^{-1}. The experimental spectrum shows a peak at 3529 cm^{-1}, corresponding to the mixed dimer where MeOH is the donor. It has previously been demonstrated that the system where *t*-BuOH is the donor is not formed in the jet expansion.[3] Our AMBER predictions are in quite good agreement with this. Indeed, for the system with MeOH as the donor, an OH-stretching wavenumber of 3529 cm^{-1} is predicted with the optimized set of charges, which is exactly the experimental value. The optimized charges show an improved frequency over set 1 and set 2 as can be seen in Table 6. The unobserved dimer with *t*-BuOH as the donor is predicted at a wavenumber of 3549 cm^{-1}, indicating a blue shift of 52 cm^{-1} with respect to the *t*-BuOH dimer, which is comparable to the 33 cm^{-1} blue shift predicted by Emmeluth et al.[3] from MP2 calculations.

The AMBER calculations are thus fully consistent with previous results, that is, we obtain a mixed-MeOH donor dimer, which is red-shifted with respect to the MeOH dimer, and a less stable mixed-*t*-BuOH donor dimer, which is blue-shifted with respect to the *t*-BuOH dimer.

5.2. MeOH/1-AdaOH. This is another mixed-alcohol dimer that does not show any torsional isomerism. Like for the previous system, two dimers can be formed. The results obtained with the AMBER force field are reported in Table 6 and are also in good agreement with our experimental results. The system where 1-AdaOH acts as the acceptor is the most stable (by about 13 kJ·mol^{-1}), and the MeOH OH-stretching band is red-shifted with respect to the MeOH dimer, for each set of charges. Once again, the AMBER calculations with the optimized charges show improved results over set 1 and set 2 and predict a red shift from the MeOH dimer of 52 cm^{-1}, while that observed experimentally is 48 cm^{-1}.

5.3. 2-AdaOH/1-AdaOH. Although only one mixed dimer has clearly been located (at 3496 cm^{-1}) in the spectrum shown in Figure 2, in which 2-AdaOH acts as the donor, we performed AMBER calculations on both dimers. The results are reported in Table 6 and are in very good agreement with our experimental results, as we nearly have a perfect match when considering the set of charges optimized to pure dimers. The system where 2-AdaOH acts as the donor is more stable by about 7 kJ·mol^{-1} in our AMBER calculations.

5.4. MeOH/1-OctOH. In this system, there remains considerable uncertainty about the 1-OctOH conformation in the

TABLE 7: MeOH/EtOH Dimers[a]

	exp[b]	set 1	set 2	opt. set	ab initio[b]
MeOH − EtOH gauche	3548	3556	3555	3546	3513
MeOH − EtOH trans	3556	3563	3566	3557	3520
EtOH gauche − MeOH	3567?	3549	3553	3559	3522
EtOH trans − MeOH	3567?	3569	3573	3570	3526

[a] Wavenumbers are given in cm^{-1}. Question marks denote a remaining experimental assignment ambiguity, which the AMBER model helps to resolve. [b] ref 3.

monomer and dimer, but the predicted red shift for the expected MeOH−1-OctOH dimer is again very close to the observed value, supporting the tentative experimental assignment of Figure 4. The inverted structure 1-OctOH−MeOH is predicted about 9 kJ·mol^{-1} higher in energy in the AMBER calculations.

5.5. MeOH/EtOH. This system is unlike the previous ones, as EtOH exists in three conformations even under supersonic jet conditions. Together with the donor/acceptor isomerism, this leads to 12 isomers, forming six pairs of enantiomers. We will focus our attention only on four of these dimers,[3] i.e., two isomers where MeOH acts as the donor and EtOH gauche/trans as an acceptor, and the other two being the isomers where MeOH acts as the acceptor. The first two dimers (MeOH−EtOH gauche and MeOH−EtOH trans) have been clearly identified in the jet FTIR spectrum,[3] while for the other two, an assignment ambiguity still remains. Our AMBER predictions are in good agreement with both the experiments and the calculations of Emmeluth et al.[3] The systems where MeOH acts as the donor are the more stable by about 7 kJ·mol^{-1}, but it is not clear which one of the trans/gauche isomers is higher in energy. The MeOH−EtOH IR spectrum shows three peaks belonging to mixed dimers located at 3567, 3556, and 3548 cm^{-1}, between the bands of pure methanol dimer (3575 cm^{-1}) and pure ethanol dimer (3532 cm^{-1}). Two of these three bands have been assigned: 3556 cm^{-1} belongs to MeOH−EtOH trans and 3548 cm^{-1} to MeOH−EtOH gauche. Table 7 shows our AMBER predictions together with both the experimental and ab initio values of Emmeluth et al.[3] When methanol acts as the donor, AMBER predicts a shift of 7−11 cm^{-1} between the trans and gauche isomers, depending on the parameter set. This is comparable to the experimental (8 cm^{-1}) and the ab initio value (7 cm^{-1}).[3] Moreover, the AMBER calculations follow the same trends as the ab initio calculations: the systems where MeOH acts as the donor are the more red-shifted, and EtOH gauche is always more red-shifted than EtOH trans. Therefore, the AMBER prediction favors the assignment of the 3567 cm^{-1} band to the EtOH trans-MeOH isomer over that to the EtOH gauche-MeOH isomer. However, this assignment must remain tentative.

The overall performance of this mixed-dimer approach is summarized in Figure 7. All six AMBER predictions fall very close to the diagonal, corresponding to a perfect match of the experimentally observed red shifts. We emphasize that these are true predictions for mixed dimers based solely on an empirical refinement of the monomer charges in pure dimers. As such, they can be more helpful in the experimental assignment than purely ab initio predictions of these subtle alkyl substitution effects. Furthermore, the predicted energy sequence for the donor/acceptor isomers of alcohol dimers agrees qualitatively with experimental observation, where available.

6. A Practical Approach

On the basis of the presented database and its analysis, we suggest the following simplified protocol to predict hydrogen-bond-induced red shifts of donor OH-stretching fundamentals in pure and mixed dimers of monofunctional, reasonably unstrained, aliphatic alcohols:

(i) Construct a Wang et al. AMBER force field[9] with standard settings for Lennard-Jones interactions, in which the OH hydrogen atoms carry a charge of +0.42 e, and the oxygen atoms carry a charge of −0.68 e.

(ii) Add −0.03 e to each oxygen for each alkyl substituent on its adjacent C atom and subtract −0.03 e if there is no such substituent (i.e., in the case of methanol).

(iii) Set all other atomic charges to zero except for the C atoms adjacent to O, which carry the charge required for monomer electroneutrality.

(iv) Minimize the dimer structure and compare its harmonic donor OH-stretching mode with that of the isolated donor molecule.

The result is predicted to be close to the experimental anharmonic red shift in the dimer, relative to a monomer of the same conformation. It may be used to guide and assist experimental assignments. If absolute wavenumbers are to be predicted, the Wang et al. AMBER OH force constant of the monomer may be slightly adjusted to reproduce the experimental monomer value. This protocol is published in the R.E.DD.B (RESP ESP charge DDataBase).[40]

Using this simplified scheme, which does not require any RESP calculation or other ab initio tool, we come back to the difficult case of ethanol dimers, where a switch in conformation upon dimerization was experimentally observed.[18] Starting from trans-EtOH, the established global minimum structure of the monomer,[41] the dimer is predicted at 3549 cm^{-1}. This value is obtained by using the universal H charge of +0.42 e, the O charge of −0.71 e for primary alcohols, and a compensating charge of +0.29 e on the adjacent C atom, together with the standard Lennard-Jones parameters of the Wang et al. force field[9] and the trans-EtOH force constant of 543 kcal·mol^{-1}·Å^{-2} which reproduces the anharmonic trans-EtOH monomer transition within 2 cm^{-1}. The predicted $(trans\text{-}EtOH)_2$ wavenumber of 3549 cm^{-1} is to be compared to the single dimer band, which survives at 3532 cm^{-1} when Ar is added to the expansion for better conformer relaxation.[18] The discrepancy of 17 cm^{-1} appears too large even for our simplified model. This supports the previous conjecture that the surviving conformer cannot be $(trans\text{-}EtOH)_2$. In a similar approach, we use the experimental[19] 1-butanol monomer vibration at ∼3680 cm^{-1} and the least red-shifted dimer donor vibration at 3552 cm^{-1} to postulate a red shift of ∼130 cm^{-1} for all-trans 1-butanol upon dimerization. Comparison to our simple model prediction of 3553 cm^{-1} suggests that our practical approach is valuable and can be used to predict red shifts.

It is for such issues that we see the largest potential of the proposed AMBER based protocol, whenever the systems become too large for high-level ab initio calculations. But even for systems as small as $(EtOH)_2$, harmonic ab initio errors in red shift predictions amount to 30 cm^{-1},[18] due to anharmonic contributions which are difficult to capture.

7. Conclusions

We have extended the set of available OH-stretching red shifts for pure and mixed aliphatic alcohol dimers using a pulsed heated nozzle coupled to an FTIR spectrometer.

This extended database was used to test the predicting power and limitations of a simplified and refined AMBER force field, as it avoids complications due to mode coupling and cooperativity.

The AMBER charge model was reduced to a single relevant parameter for aliphatic alcohols, and the pure alcohol dimers were used as a training set for this charge parameter, which behaved in a physically meaningful way. Subsequently, our experimental results for mixed-alcohol dimers were used to test the reparametrization. It turns out that subtle chiral recognition effects, which have been recently uncovered for ethanol,[18,39] are not captured. However, electronic and steric effects as well as the general spread of red shifts due to conformational isomerism are captured remarkably well. On the basis of data for pure dimers, mixed-dimer absorptions can be reliably predicted. We propose a simplified protocol which allows for the prediction of OH-stretching red shifts for dimers of monofunctional unstrained aliphatic alcohols without the need for ab initio charge calculations. Our semiempirical approach turns out to be valuable in cases where accurate ab initio calculations are out of reach and as an independent assessment where they are available. It will be interesting to extend the proposed analysis to mixed alcohol−ether complexes.[42] However, the approach may not be easily generalized to multifunctional, aromatic, and cooperative systems or to other properties such as absolute binding energies.

Acknowledgment. We thank D. Zimmermann for his early contributions to the dimer spectra of some alcohols. We are grateful to the referees for valuable comments helping in the extension and assessment of the AMBER model. Support by the DFG research training group GRK782 and by the Fonds der Chemischen Industrie is gratefully acknowledged.

References and Notes

(1) Barnes, A. J.; Hallam, H. E.; Jones, D. *Proc. R. Soc. London, Ser. A* **1973**, *335*, 97.
(2) Smith, F. A.; Creitz, E. C. *J. Res. Natl. Bur. Stand. (U.S.)* **1951**, *46*, 145.
(3) Emmeluth, C.; Dyczmons, V.; Suhm, M. A. *J. Phys. Chem. A* **2006**, *110*, 2906.
(4) Häber, T.; Schmitt, U.; Suhm, M. A. *Phys. Chem. Chem. Phys.* **1999**, *1*, 5573.
(5) Luckhaus, D.; Quack, M.; Schmitt, U.; Suhm, M. A. *Ber. Bunsen-Ges. Phys. Chem.* **1995**, *99*, 457.
(6) Bakke, J. M.; Bjerkeseth, L. H. *J. Mol. Struct.* **1997**, *407*, 27.
(7) Coussan, S.; Roubin, P.; Perchard, J. P. *J. Phys. Chem. A* **2004**, *108*, 7331.
(8) Lutz, B. T. G.; Van der Maas, J. H. *J. Mol. Struct.* **1997**, *436*−*437*, 213.
(9) Wang, J. M.; Cieplak, P.; Kollman, P. A. *J. Comput. Chem.* **2000**, *21*, 1049.
(10) Wang, J. M.; Kollman, P. A. *J. Comput. Chem.* **2001**, *22*, 1219.
(11) Derreumaux, P.; Dauchez, M.; Vergoten, G. *J. Mol. Struct.* **1993**, *295*, 203.
(12) Derreumaux, P.; Lagant, P.; Vergoten, G. *J. Mol. Struct.* **1993**, *295*, 223.
(13) Derreumaux, P.; Vergoten, G. *J. Mol. Struct.* **1993**, *295*, 233.
(14) Tristram, F.; Durier, V.; Vergoten, G. *J. Mol. Struct.* **1996**, *378*, 249.
(15) Buck, U.; Siebers, J. G. *Eur. Phys. J. D* **1998**, *1*, 207.
(16) Jorgensen, W. L. *J. Phys. Chem.* **1986**, *90*, 1276.
(17) Schlegel, H. B.; Wolfe, S. *J. Chem. Phys.* **1977**, *67*, 4181.
(18) Emmeluth, C.; Dyczmons, V.; Kinzel, T.; Botschwina, P.; Suhm, M. A.; Yanez, M. *Phys. Chem. Chem. Phys.* **2005**, *7*, 991.
(19) Provencal, R. A.; Casaes, R. N.; Roth, K.; Paul, J. B.; Chapo, C. N.; Saykally, R. J.; Tschumper, G. S.; Schaefer, H. F. *J. Phys. Chem. A* **2000**, *104*, 1423.
(20) Zimmermann, D.; Häber, T.; Schaal, H.; Suhm, M. A. *Mol. Phys.* **2001**, *99*, 413.
(21) Schaal, H.; Häber, T.; Suhm, M. A. *J. Phys. Chem. A* **2000**, *104*, 265.
(22) Zimmermann, D. Diplom Thesis. Georg-August Universität, Göttingen, 2000.
(23) Rice, C. A.; Borho, N.; Suhm, M. A. *Z. Phys. Chem.* **2005**, *219*, 379.
(24) Case, D. A.; Darden, T. A.; Cheatham, III, T. E.; Simmerling, C. L.; Wang, J.; Duke, R. E.; Luo, R.; Merz, K. M.; Wang, B.; Pearlman, D. A.; Crowley, M.; Brozell, S.; Tsui, V.; Gohlke, H.; Mongan, J.; Hornak, V.; Cui, G.; Beroza, P.; Schafmeister, C.; Caldwell, J. W.; Ross, W. S.; Kollman, P. A. *AMBER 8*; University of California: San Francisco, 2004.
(25) Wang, J. M.; Wolf, R. M.; Caldwell, J. W.; Kollman, P. A.; Case, D. A. *J. Comput. Chem.* **2004**, *25*, 1157.
(26) Frisch, M. J.; Trucks, G. W.; Schlegel, H. B.; Scuseria, G. E.; Robb, M. A.; Cheeseman, J. R.; Montgomery, J. A., Jr.; Vreven, T.; Kudin, K. N.; Burant, J. C.; Millam, J. M.; Iyengar, S. S.; Tomasi, J.; Barone, V.; Mennucci, B.; Cossi, M.; Scalmani, G.; Rega, N.; Petersson, G. A.; Nakatsuji, H.; Hada, M.; Ehara, M.; Toyota, K.; Fukuda, R.; Hasegawa, J.; Ishida, M.; Nakajima, T.; Honda, Y.; Kitao, O.; Nakai, H.; Klene, M.; Li, X.; Knox, J. E.; Hratchian, H. P.; Cross, J. B.; Bakken, V.; Adamo, C.; Jaramillo, J.; Gomperts, R.; Stratmann, R. E.; Yazyev, O.; Austin, A. J.; Cammi, R.; Pomelli, C.; Ochterski, J. W.; Ayala, P. Y.; Morokuma, K.; Voth, G. A.; Salvador, P.; Dannenberg, J. J.; Zakrzewski, V. G.; Dapprich, S.; Daniels, A. D.; Strain, M. C.; Farkas, O.; Malick, D. K.; Rabuck, A. D.; Raghavachari, K.; Foresman, J. B.; Ortiz, J. V.; Cui, Q.; Baboul, A. G.; Clifford, S.; Cioslowski, J.; Stefanov, B. B.; Liu, G.; Liashenko, A.; Piskorz, P.; Komaromi, I.; Martin, R. L.; Fox, D. J.; Keith, T.; Al-Laham, M. A.; Peng, C. Y.; Nanayakkara, A.; Challacombe, M.; Gill, P. M. W.; Johnson, B.; Chen, W.; Wong, M. W.; Gonzalez, C.; Pople, J. A. *Gaussian 03*, revision C.02; Gaussian, Inc.: Wallingford, CT, 2004.
(27) Cornell, W. D.; Cieplak, P.; Bayly, C. I.; Kollman, P. A. *J. Am. Chem. Soc.* **1993**, *115*, 9620.
(28) Bayly, C. I.; Cieplak, P.; Cornell, W. D.; Kollman, P. A. *J. Phys. Chem.* **1993**, *97*, 10269.
(29) Cieplak, P.; Cornell, W. D.; Bayly, C.; Kollman, P. A. *J. Comput. Chem.* **1995**, *16*, 1357.
(30) Schmidt, M. W.; Baldridge, K. K.; Boatz, J. A.; Elbert, S. T.; Gordon, M. S.; Jensen, J. H.; Koseki, S.; Matsunaga, N.; Nguyen, K. A.; Su, S. J.; Windus, T. L.; Dupuis, M.; Montgomery, J. A. *J. Comput. Chem.* **1993**, *14*, 1347.
(31) Cieplak, P.; Caldwell, J.; Kollman, P. *J. Comput. Chem.* **2001**, *22*, 1048.
(32) Weiner, S. J.; Kollman, P. A.; Nguyen, D. T.; Case, D. A. *J. Comput. Chem*. **1986**, *7*, 230.
(33) Durig, J. R.; Cox, F. O.; Groner, P.; Van der Veken, B. J. *J. Phys. Chem.* **1987**, *91*, 3211.
(34) Liu, S.; Dykstra, C. E. *J. Phys. Chem.* **1986**, *90*, 3097.
(35) Hagemeister, F. C.; Gruenloh, C. J.; Zwier, T. S. *J. Phys. Chem. A* **1998**, *102*, 82.
(36) Bizzarri, A.; Stolte, S.; Reuss, J.; Van Duijneveldt-van De Rijdt, J. G. C. M.; Van Duijneveldt, F. B. *Chem. Phys.* **1990**, *143*, 423.
(37) Coussan, S.; Bouteiller, Y.; Perchard, J. P.; Zheng, W. Q. *J. Phys. Chem. A* **1998**, *102*, 5789.
(38) Fang, H. L.; Swofford, R. L. *Chem. Phys. Lett.* **1984**, *105*, 5.
(39) Hearn, J. P. I.; Cobley, R. V.; Howard, B. J. *J. Chem. Phys.* **2005**, 123.
(40) Dupradeau, F.-Y.; Lelong, R.; Stanislawiak, E.; Delepine, J. C.; Pecher, J.; Cieplak, P. The RESP ESP charge DDataBase; Université de Picardie Jules Verne, Amiens, France − Burnham Institute for Medical Research, La Jolla, CA, 2006.
(41) Quade, C. R. *J. Mol. Spectrosc.* **2000**, *203*, 200.
(42) Raveendran, P.; Zimmermann, D.; Häber, T.; Suhm, M. A. *Phys. Chem. Chem. Phys.* **2000**, *2*, 3555.
(43) Hunt, R. H.; Shelton, W. N.; Flaherty, F. A.; Cook, W. B. *J. Mol. Spectrosc.* **1998**, *192*, 277.